Electronic Supplementary Information

Introduction of antifouling photoelectrode: an effective strategy for high-performance photoelectrochemical cytosensor

Linzheng Ma[ab], Huan Zhao[a], Gao-Chao Fan*[a], Xiliang Luo*[a] and Jun-Jie Zhu*[b]

[a] Key Laboratory of Optic-electric Sensing and Analytical Chemistry for Life Science, MOE; Shandong Key Laboratory of Biochemical Analysis; College of Chemistry and Molecular Engineering, Qingdao University of Science and Technology, Qingdao 266042, China

[b] State Key Laboratory of Analytical Chemistry for Life Science, School of Chemistry and Chemical Engineering, Nanjing University, Nanjing 210093, China

*E-mail: gcfan@qust.edu.cn; xiliangluo@qust.edu.cn; jjzhu@nju.edu.cn

Section 1: Experimental

Materials and Reagents. Glycidol, methanol, acetone, zinc nitrate, hexamine, stannous chloride ($SnCl_2$), lithium perchlorate ($LiClO_4$), sodium methoxide, ethylene glycol, polyvinyl pyrrolidone (PVP), thioacetamide, 1,1-carbonyldiimidazole (CDI), and fluorescein diacetate were obtained from Aladdin reagent Inc. (Shanghai, China). Dulbecco's modified Eagle's medium (DMEM) and 1,4-dioxane, (2,3-dihydrothieno[3,4-b][1,4] dioxin-2-yl)methanol (EDOT-MeOH) were purchased from Sigma-Aldrich (Beijing, China). Human serum albumin (HSA), carcinoembryonic antigen (CEA), and α-fetoprotein (AFP) were obtained from Shanghai Linc-Bio Science Co. Ltd. (China). AS1411 aptamer sequence (5'-NH_2-$(CH_2)_6$-TTT TGG TGG TGG TGG TTG TGG TGG TGG TGG-3') was synthesized by Shanghai Songong Biotechnology Co., Ltd. (Shanghai, China). Human cervical carcinoma cells (HeLa) was purchased from Ocean University of China (Qingdao, China). Ascorbic acid (AA) was purchased from Sinopharm Chemical Reagent Co., Ltd (China). Phosphate buffered saline (PBS, 0.1 M, pH 7.4) were used throughout all experiments. All aqueous solutions were prepared using deionized water (DI water, 18 MΩ/cm) produced by a Milli-Q water purifying system.

Apparatus. Field-emission scanning electron microscopy (FE-SEM) was carried out on a Hitachi S-4800 scanning electron microscope (Hitachi Co., Japan). PEC measurements were performed with a homemade PEC system. A 150 W Xenon lamp was utilized as the irradiation source with the light intensity of 300 $mW \cdot cm^{-2}$ estimated by a radiometer (Photoelectric Instrument of Beijing Saifan Co., LTD.). Photocurrent output was measured on a CHI 760D electrochemical workstation (Shanghai Chenhua Apparatus Corporation, China). X-ray photoelectron spectroscopy (XPS) was performed using an ESCALAB 250Xi spectrometer (Thermo Fisher Scientific, UK) with a monochromatic Al Kα X-ray source, and all spectra were calibrated by normalizing the C (1s) peak to the standard value of 284.6 eV. Electrochemical impedance spectroscopy (EIS) was carried out on an Autolab potentiostat/galvanostat (PGSTAT 30, Eco Chemie B.V., Utrecht, Netherlands) with a three-electrode system in 0.1 M KCl solution containing 5.0 mM $K_3[Fe(CN)_6]/K_4[Fe(CN)_6]$ (1:1) mixture as a redox probe and recorded in the frequency range of 0.01 Hz-100 kHz with an amplitude of 50 mV. Hydrophilicity tests of different modified surfaces with static water contact angle were carried out with the JC2000 Instrument (Shanghai Zhongchen Instrument Co., China). Cell morphology were visualized and imaged with an Olympus IX81 fluorescence microscope (Olympus, Japan) equipped with a FITC

filter at 4x or 10x magnification. All the nuclear magnetic resonance (NMR) experiments were recorded using a Bruker AVANCE-Ⅲ 600 MHz NMR spectrometer with a total sample volume of nearly 500 μL taken in a Φ5 mm NMR tube, and this experimentation was conducted at 298 K.

Synthesis of the monomer. The monomer ((2,3-dihydrothieno[3.4-b][1,4]dioxin-2-yl)methoxy) ethane-1,2-diol of the PEDOT-HPG was prepared using an anionic ring opening reaction of glycidol on the EDOT-MeOH [1,2], with 1,4-dioxane as the reaction medium and sodium methoxide as the catalyst. Typically, EDOT-MeOH (10 mM) and sodium methoxide (20 mM) were dissolved with methanol in a three-neck flask. In order to remove excess methanol, the mixture was stirred for 2 h at 90 °C to obtain sodium alkoxide. As it was cooled, 20 mL of 1,4-dioxane was added into the three-neck flask and subsequently sonication for 20 min until a homogenous solution was obtained. The obtained solution was subsequently degassed for 10 min with nitrogen gas to remove dissolved oxygen and store in an inert gases protected condition. Afterwards, the solution was kept at 95 °C to proceed the reaction with glycidol under the stirring. Glycidol was slowly dropwise added into the flask with nitrogen protection and vigorous stirring for 12 h, choosing the initiator amount according to the monomer/initiator ratio. After naturally cooled to room temperature, the solution was filtered and concentrated with a rotary evaporator to collect ((2,3-dihydrothieno[3.4-b][1,4]dioxin-2-yl)methoxy) ethane-1,2-diol as a liquid. The synthesized monomer was characterized using ^{1}H and ^{13}C nuclear magnetic resonance (NMR) spectroscopy (see Fig. S1).

Synthesis of ZnO-NTs. Before the formation of ZnO nanotubes (ZnO-NTs), ZnO nanorods (ZnO-NRs) were firstly formed on an ITO-glass by electrochemical deposition [3]. It was performed on a CHI 760D electrochemical workstation with a three-electrode cell consist of a Pt-wire counter electrode, an Ag/AgCl reference electrode and an ITO-glass working electrode. Briefly, ZnO-NRs were electrodeposited in an aqueous solution containing 6.3 mM zinc nitrate and 6.3 mM hexamine. The growth was performed at 80 °C with an applied potential of 1.0 V. To obtain the ZnO-NTs, the as-prepared ZnO-NRs was immersed in 0.3 M KOH aqueous solution at 80 ℃ for 60 min for chemical etching [4]. The substrate was then taken out from the solution, washed with DI water, and followed by drying with pure N_2 stream. Finally, the ZnO-NTs modified ITO electrode was acquired.

Growth of SnS nanosheets on ZnO-NTs. The growth of SnS on ZnO-NTs was similar to the previous literature [5]. Typically, 1.0 g of PVP (M.W. 24000) were first ultrasonically dispersed into 50

mL of ethylene glycol. After that, 1.6 mL of ethylene glycol solution containing 0.64 mmol of $SnCl_2$ and 1.6 mL of ethylene glycol solution containing 0.64 mmol of thioacetamide were added into the above solution. Then, the ZnO-NTs modified ITO electrode was placed in the mixed solution above and were transferred into a sealed Teflon-lined stainless-steel autoclave. After kept at 160 ℃ for 12 h, the resulting electrode was rinsed with ethanol and water, and the SnS/ZnO-NTs modified ITO electrode was acquired.

Deposition of PEDOT-HPG on SnS/ZnO-NTs. The polymerization of PEDOT-HPG onto the surface of the SnS/ZnO-NTs electrode was similar with previous literature [6]. It was performed on a CHI 760D electrochemical workstation with a three-electrode cell consist of an Ag/AgCl reference electrode, a Pt-wire as counter electrode and SnS/ZnO-NTs modified ITO electrode as working electrode. The working electrode surface was exposed to both the electrolyte and the irradiation, and the optical path of the irradiation source was kept still in the whole process. The monomer is hydrophilic, and it was polymerized in aqueous solution. The polymerization solution contained 100 mM $LiClO_4$ and 60 mM monomer in DI water, which was deaerated by pure nitrogen gas for 15 min prior to polymerization. The chronoamperometry technique was utilized and the PEDOT-HPG layer was polymerized on the SnS/ZnO-NTs electrode at 1.0 V for 90 s. Simultaneously with the start of the potentiodynamic polymerization, the working electrode was irradiated. Eventually, the desired PEDOT-HPG/SnS/ZnO-NTs photoelectrode was obtained.

Fabrication of the PEC cytosensor. Amino functionalized AS1411 aptamer was covalentlybound on the surface of the PEDOT-HPG/SnS/ZnO-NTs photoelectrode with 1,1-carbonyldiimidazole (CDI) as cross-linking agent [7,8]. Typically, 20 μL of 30 mg/mL CDI aqueous solution was scattered on the photoelectrode and kept at room temperature for overnight, which activated the hydroxyl groups of PEDOT-HPG on the photoelectrode. After activation step, the electrode was washed with DI water and incubated with 20 μL of 2 μM AS1411 aptamer for 12 h. Finally, the fabricated cytosensor were fully rinsed and stored in PBS (10 mM, pH 7.4) at 4 ℃ until use.

Cell culture. The HeLa cells were cultured in an RPMI-1640 medium (Gibco, Grand Island, NY) supplemented with 10% fetal bovine serum (FBS), streptomycin (100 μg/mL), and penicillin (100 μg/mL) at 37 °C under 5% CO_2 atmosphere. At logarithmic growth phase, the cells were collected and separated from the medium by centrifugation at 1000 rpm for 5 min, and then washed with Dulbecco's

phosphate-bu□ered saline (D-PBS). The cell sediment was resuspended in D-PBS to acquire a homogeneous suspension. The cell number was determined by a Petroff–Hausser cell counter.

PEC detection. The prepared cytosensor was incubated in 1 mL of 10 mM PBS buffer containing different concentrations of HeLa cells at 37 °C for 1 h. After the incubation step, the PEC cytosensor was taken out and gently rinsed with sterilized PBS. The PEC measurements were performed in a three-electrode system: Ag/AgCl electrode as reference electrode, Pt wire as counter electrode and the cytosensor as working electrode. The photocurrent test was performed in PBS (pH 7.4, 0.1 M) containing 0.1 M ascorbic acid (AA), which acted as electron donors of the photoelectrode. A xenon lamp with a spectral range of 300-2500 nm was utilized as irradiation source, and it was switched on and off every 10 s. The applied voltage was 0.0 V.

Section 2: ^{1}H NMR and ^{13}C NMR of the monomer

All the nuclear magnetic resonance (NMR) experiments were recorded using a Bruker AVANCE-Ⅲ 600 MHz NMR spectrometer with a total sample volume of nearly 500 μL taken in a Φ5 mm NMR tube. And this experimentation was conducted at 298 K. Monomer: 1H NMR (300 MHz, CDCl3) δ 6.30-6.36 (m, 2H), 4.20-4.30 (m, 2H), 3.90-3.97 (m, 1H), 3.65-3.71 (m, 2H), 4.40-4.50(w, 1H), 3.10-3.22 (m, 2H), as shown in Fig. S1A. Monomer: 13C NMR (75 MHz, CDCl3) δ 141.84, 103.12, 99.90, 99.55, 73.95, 67.52, 64.5, as shown in Fig. S1B.

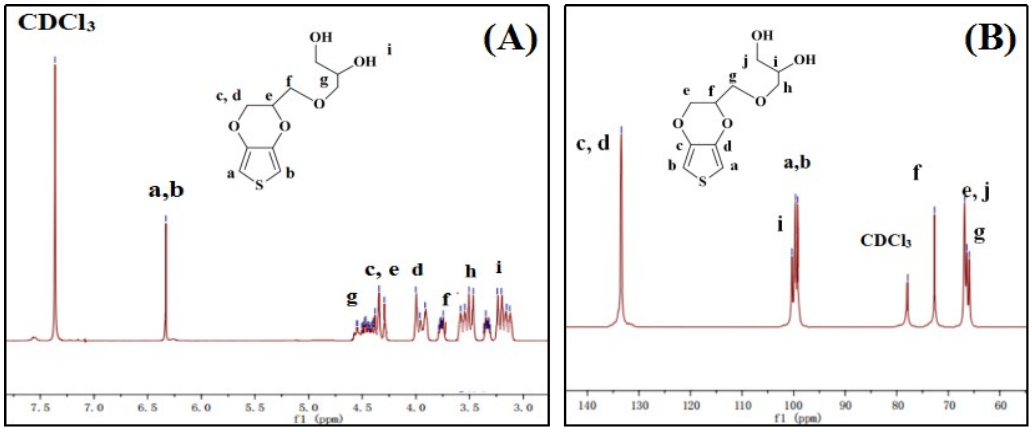

Fig. S1. The ^{1}H NMR (A) and ^{13}C NMR (B) of the monomer of PEDOT-HPG.

Section 3: XPS characterization of the photoelectrode.

In order to further confirm the elements states and composition information, XPS of the PEDOT-HPG/SnS/ZnO-NTs photoelectrode during its fabrication process was characterized, as shown in in Fig. S2. It is observed in Panel A that the ZnO-NTs was mainly composed of Zn and O elements, and the XPS peak for C 1s was used as the internal reference to correct the binding energy. After SnS layer deposition, the typical XPS peaks of S 2p and Sn 3d appeared (Panel B). While PEDOT-HPG layer modification, as shown in Panel C, the typical XPS peaks for Cl 2p arise, and the Cl element was derived from the raw materials of $LiClO_4$ in the polymerization process. Thus, the XPS further proved successful fabrication of the PEDOT-HPG/SnS/ZnO-NTs photoelectrode.

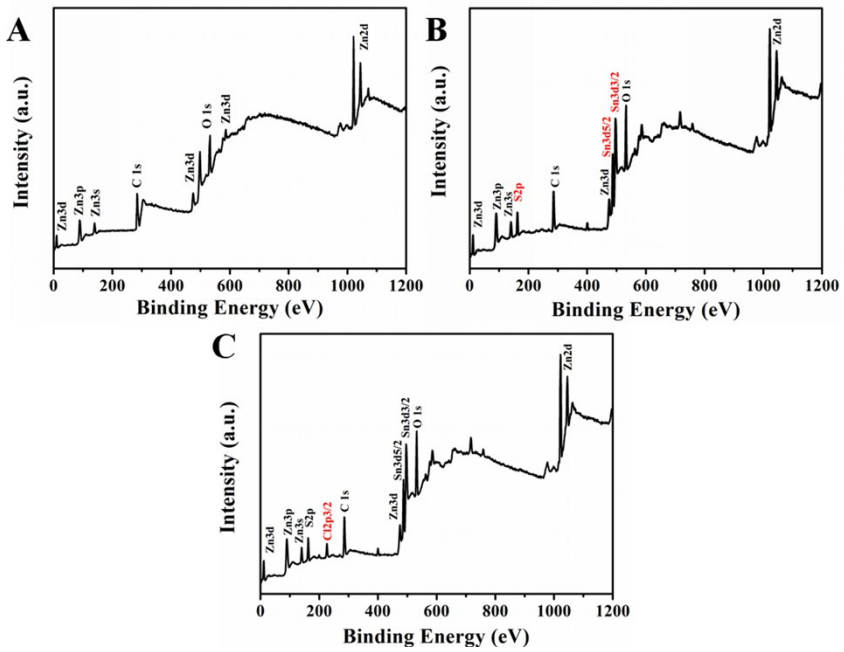

Fig. S2. Full-scan XPS spectra of the electrodes: (A) ZnO-NTs, (B) SnS/ZnO-NTs, and (C) PEDOT-HPG/SnS/ZnO-NTs.

Section 4: Optimal conditions of the photoelectrode

Fig. S3A shows photocurrent responses of the ZnO-NTs electrode prepared with different etching time of ZnO-NRs. Along with increase in etching time, the photocurrent response of the ZnO-NTs electrode increased, which was because the enlarged specific area of ZnO-NTs could supply more active sites for charge transfer. It could be observed that the photocurrent intensity reached its maximum when the etching time was 2.5 h. After further increase of etching time, the photocurrent decreased due to structural failure caused by excessive etching. Fig. S3B displays photocurrent responses of the SnS/ZnO-NTs electrode prepared with different deposition time of SnS. As the

deposition time of SnS increased initially, the deposition amount of SnS on the ZnO-NTs accumulated resulting in the enhanced photocurrent intensity, and the peak photocurrent was reached at the deposition time of 12 h. The photocurrent intensity decreased as the deposition time continued to increase, which was because the excessively deposited SnS would acted as surface recombination sites to enlarge the diffusion resistance of the electron motion [9]. Thus, 12 h was selected as the optimal time for SnS deposition. Fig. S3C exhibits photocurrent responses of the PEDOT-HPG/SnS/ZnO-NTs photoelectrode prepared with different polymerization time. As the polymerization time of PEDOT-HPG increased to 90 s, the photocurrent intensity increased gradually to a peak. After further increase in the polymerization time, the photocurrent intensity decreased, owing to the reduced light absorption from excessive PEDOT-HPG coating on the photoelectrode [10, 11]. Therefore, the optimal polymerization time was selected as 90 s. Fig. S3D describes photocurrent responses of the aptamer modified photoelectrode with varied concentrations of aptamer. With increase in the concentration of aptamer, the photocurrent decreased gradually and reached nearly a plateau while the concentration was 2.0 μM, implying that abundant aptamer probe were immobilized on the electrode. As a result, 2.0 μM of aptamer probe was utilized to modify the photoelectrode.

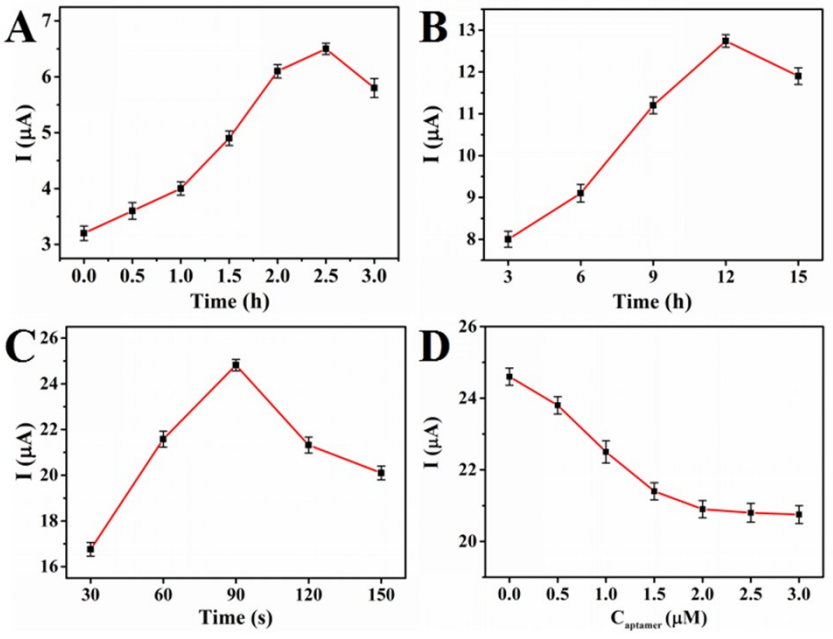

Fig. S3. Photocurrent responses of the (A) ZnO-NTs electrode with different etching time, (B) SnS/ZnO-NTs electrode with different deposition time of SnS, (C) PEDOT-HPG/SnS/ZnO-NTs photoelectrode with different polymerization time of PEDOT-HPG, and (D) aptamer modified photoelectrode with varied concentrations of aptamer.

Section 5: Calculation of energy levels of PEDOT-HPG

The energy levels of PEDOT-HPG were calculated according to the previous paper [12-14]. To determine energy gap (E_g) of the sample, UV−vis absorption spectrum of the PEDOT-HPG was first performed, as shown in Fig. S4A. The E_g of the PEDOT-HPG was then calculated to be 1.60 eV by the onset wavelength (λ_{onset}) of 775 nm according to Eq. 1:

$$E_g\ (eV) = 1240 / \lambda_{onset}\ (nm) \quad (1)$$

$$IP = -(4.80 - E_{1/2}^{Fc/Fc+} + E_{ox}) \quad (2)$$

$$EA = IP + E_g \quad (3)$$

The LUMO and HOMO energy levels of PEDOT-HPG can be obtained by calculating their electron affinity (EA) and ionization potential (IP). The redox potentials were referenced against ferrocene/ferrocenium (Fc/Fc+) couple and their potential absolute energy level was 4.80 eV in Vacuum. The $E_{1/2}^{Fc/Fc+}$ of bare ITO was determined as +0.32 V with the scan rate of 50 mV/s in 0.5 mM Fc solution. E_{ox} is the oxidation initiation potential, and the E_{ox} of PEDOT-HPG was calculated as 0.93 eV from Fig. S4B. The IP of the PEDOT-HPG complied to Eq. 2, and it was calculated to be −5.41 eV using E_{ox} value of 0.93 V. The EA was then calculated as −3.81 eV by Eqs. 1 and 3. Thus, the LUMO/ HOMO was calculated as −3.81 eV/−5.41 eV for PEDOT-HPG.

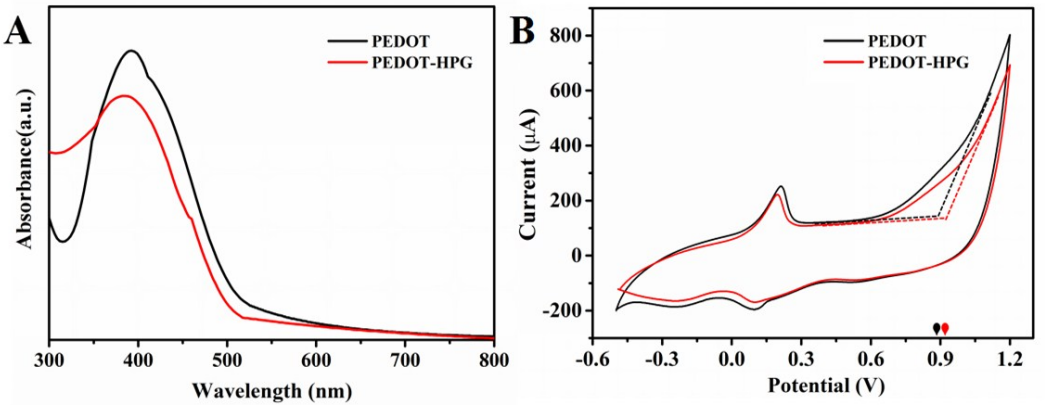

Fig. S4. (A) UV−vis absorption of PEDOT (black line) and PEDOT-HPG (red line); (B) CVs of the ITO glass modified by PEDOT (black line) and PEDOT-HPG (red line) in a deoxygenated anhydrous acetonitrile solution of tetrabutylammonium hexafluorophosphate (0.1 M) at scan rate of 50 mV/s.

Section 6: EIS test on antifouling property

The antifouling property of the PEDOT-HPG/SnS/ZnO-NTs was further characterized by EIS and photocurrent response. Fig. S5A exhibits electrochemical impedance spectroscopy (EIS) of the PEDOT-HPG/SnS/ZnO-NTs photoelectrode after incubated in different diluted human plasma solutions, and it can be seen that there was only small electron-transfer resistance (R_{et}) change until the concentration was increased to 10%. For the purpose of comparison, EIS of the SnS/ZnO-NTs electrode was also recorded, as shown in Fig. S5B. The control experiment showed that there was obvious change in R_{et} after the SnS/ZnO-NTs electrode incubated in serum, even for 1% of the diluted human plasma, implying evident nonspecific adsorption of the SnS/ZnO-NTs electrode. The results also confirmed the PEDOT-HPG modified photoelectrode possessed excellent antifouling capability to resist the nonspecific adsorption even in complex biological media.

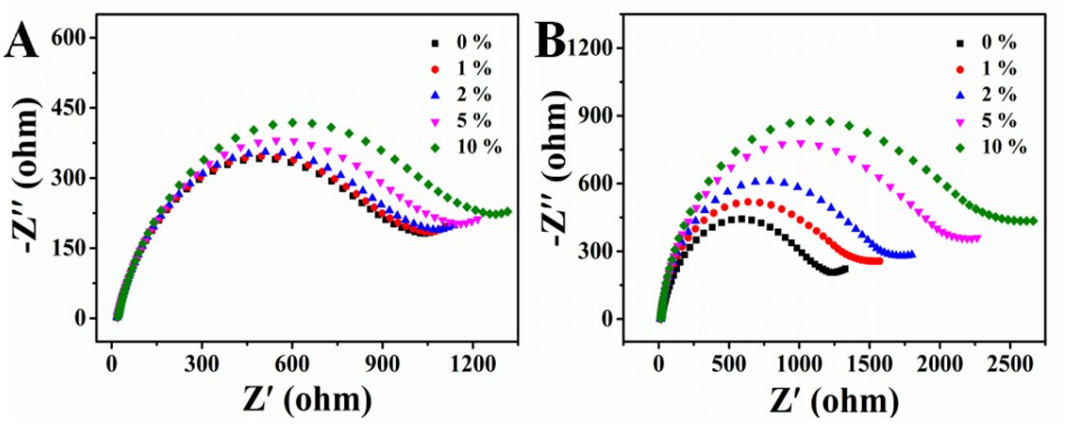

Fig. S5. EIS of the (A) PEDOT-HPG/SnS/ZnO-NTs and (B) SnS/ZnO-NTs electrodes after incubated in different concentrations of diluted human plasma solutions.

Section 7: References

1. Sunder, A., Hanselmann, R., Frey, H., Mulhaupt, R., *Macromolecules* 1999, **32**, 4240−4246.
2. Cucciniello, R., Ricciardi, M., Vitiello, R., Di Serio, M., Proto, A., Capacchione, C., *ChemSusChem* 2016, **9**, 3272–3275.
3. Cui, J., and Gibson U.J., *J. Phys. Chem. B* 2005, **109**, 22074–22077.
4. Chu, D., Masuda, Y., Ohji, T., Kato, K., *J. Am. Ceram. Soc.* 2010, **93**, 887–893.
5. He, P.L., Fang, Y.J., Yu, X.Y., Lou, X.W., *Angew. Chem. Int. Ed.* 2017, **56**, 12202–12205.
6. Samu, G.F., Visy, C., Rajeshwar, K., Sarker, S., Subramanian, V.R., Janáky, C., *Electrochim. Acta* 2015, **151**, 467−476.

7. Soylemez, S., Hacioglu, S.O., Kesik, M., Unay, H., Cirpan, A., Toppare, L., *ACS Appl. Mater. Interfaces* 2014, **6**, 18290−18300.
8. Korogiannaki, M., Samsom, M., Schmidt, T.A., Sheardown, H., *ACS Appl. Mater. Interfaces* 2018, **10**, 30125−30136.
9. Fan, G.C., Ren, X.L., Zhu, C., Zhang, J.R., Zhu, J.J. *Biosens. Bioelectron.* 2014, **59**, 45–53.
10. Chong, B., Zhu, W., Hou, X., *J. Mater. Chem. A*, 2017, **5**, 6233–6244.
11. Fan, G.C., Ma, L., Jayachandran, S., Li, Z., Luo X., *Chem. Commun.* 2018, **54**, 7062–7065.
12. Ma, L., Fan, G.C., Jayachandran, S., Liu, Q., Li, Z., Luo, X., *Sensors Actuators, B Chem.* 2019, **283**, 705–713.
13. Dissanayake, D.M.N.M., Lutz, T., Curry, R.J., Silva, S.R.P., *Appl. Phys. Lett.* 2008, **93**, 043501–043503.
14. Li, S.G., Yuan, Z.C., Deng, P., Sun, B.B., Zhang, Q., *Polym. Chem.* 2014, **5**, 2561–2566.